Structural and Biochemical Properties of Bidentate Tetraaquarhodium(III) Complexes of Inorganic Pyrophosphate and Adenosine 5′-Diphosphate†

Andrew L. Shorter,‡ Tuli P. Haromy,§ Theresa Scalzo-Brush,‡ Wilson B. Knight,‡,∥ Debra Dunaway-Mariano,*,‡ and Muttaiya Sundaralingam*,§

Department of Chemistry and Biochemistry, University of Maryland, College Park, Maryland 20742, and Department of Biochemistry, College of Agricultural and Life Sciences, University of Wisconsin—Madison, Madison, Wisconsin 53706

Received June 26, 1986; Revised Manuscript Received October 14, 1986

ABSTRACT: The structural and biochemical properties of the α,β-bidentate tetraaquarhodium(III) complexes of inorganic pyrophosphate [$Rh(H_2O)_4PP$] and adenosine diphosphate [$Rh(H_2O)_4ADP$] are examined. These Rh(III) complexes are exchange-inert analogues of the corresponding physiologically important $Mg^{II}PP$ and $Mg^{II}ADP$ complexes. The crystal structure of $[Rh(H_2O)_4H_2P_2O_7]^+Cl^-$ shows that the six-membered chelate ring adopts a twist-boat conformation with an unusually high puckering amplitude of 0.756 (3) Å. The Rh coordination distances average 2.02 (1) Å, while the bridge P–O bonds are virtually equal in length. All 10 protons of the complex participate in hydrogen bonding. There are two intramolecular hydrogen bonds between the phosphate oxygen atoms and the axially coordinated water molecules. The $Rh(H_2O)_4PP$ complex was found to be a substrate for yeast inorganic pyrophosphatase, with K_i = 0.063 (7) mM and V_m = 500 (100) min^{-1}. The two screw sense isomers of $Rh(H_2O)_4ADP$ were prepared from (R_P)-[α-$^{16}O,^{18}O$]ADP and assigned configuration on the basis of the magnitude of their ^{31}P NMR isotopic chemical shifts. The $Rh(H_2O)_4ADP$ complex binds a number of kinases as tightly as MgADP. Arginine kinase and creatine kinase were shown to bind the Δ $Rh(H_2O)_4ADP$ isomer 7 and 45 times tighter, respectively, than the Λ isomer. The reactivity of $Rh(H_2O)_4PP$ with pyrophosphatase is comparable to that of $Cr(H_2O)_4PP$, and the binding affinities of the $Rh(H_2O)_4ADP$ screw sense isomers for kinases are also comparable to those observed for the corresponding $Cr(H_2O)_4ADP$ screw sense isomers.

ATP,[1] ADP, PP, and other di- and triphosphates are usually found in the cell as the Mg(II) complexes. In most instances the Mg(II) complex participates in biochemical processes rather than the uncomplexed species. Mg(II) reversibly binds to polyphosphates at more than one position, and for this reason Mg(II)–polyphosphate complexes exist in solution as mixtures of stereoisomers and/or structural isomers. A fundamental step in defining a Mg(II)–polyphosphate-dependent process is to determine which isomer is selected from the mixture in solution. For example, an enzyme may bind all of the isomers of a given Mg(II) complex, but only one of these isomers may be bound in the correct orientation for catalysis. Unfortunately, owing to the rapid ligand-exchange rates and the lack of useful spectral properties of the Mg(II) ion in these complexes, meaningful studies of the Mg(II)–polyphosphate are rarely possible. An alternate approach to investigate the properties of these complexes is to substitute "exchange-inert" metal ions [viz., Co(III), Cr(III), Rh(III), Ir(III), or Ru(III)] for Mg(II). The relatively stable M(III)–polyphosphate complexes are suitable for a variety of structure/activity studies which can provide insight into the properties of the physiologically important Mg(II)–polyphosphate complexes.

Previous efforts have focused on Co(III)– and Cr(III)–polyphosphate complexes (Cleland, 1985; Dunaway-Mariano, 1985; Sundaralingam & Haromy, 1985). While these complexes have proved generally useful in studies of the structural and chemical properties of the metal–polyphosphate complexes, they do possess certain properties that severely limit their application in biochemical studies. The Co(III) complexes, for example, must be stabilized by ammine ligands. Only a few enzymes have been identified that will even bind these complexes. The Cr(III)–polyphosphate complexes are, on the other hand, difficult to characterize. With the exception of Cr(III)–pyrophosphate complexes (Merritt et al., 1981; Haromy et al., 1984; Linck et al., 1986), Cr(III)–polyphosphate complexes have not been obtained in crystalline form. Consequently, structure assignment by X-ray crystallographic analysis has not been possible. Moreover, NMR-based structural analysis of the Cr(III) complexes is precluded by the paramagnetic properties of the metal ion. The Rh(III) ion not only forms a stable tetraaqua chelate complex but also is diamagnetic, which facilitates its use for NMR investigations. For this reason and also to extend the series of exchange-inert metal–polyphosphate complexes available for structure/activity studies, we have directed our attention to

† This work was supported in part by National Institutes of Health Grant GM-17378 to M.S. and by National Institutes of Health Grant GM-28688 and American Heart Association Grant 83918 to D.D.-M. D.D.-M. acknowledges Research Career Development Award ES-00111 from the National Institutes of Health and a Fellowship Award from the Alfred P. Sloan Foundation. A.L.S. and W.B.K. acknowledge Postdoctoral Fellowship Awards from the Maryland Chapter of the American Heart Association.

* Address correspondence to either author.

‡ University of Maryland.

§ University of Wisconsin—Madison.

∥ Present address: Department of Biochemistry, University of Wisconsin—Madison, Madison, WI 53706.

[1] Abbreviations: EDTA, ethylenediaminetetraacetic acid; CDTA, *trans*-1,2-diaminocyclohexane-*N*,*N*,*N*′,*N*′-tetraacetic acid; ATP, adenosine 5′-triphosphate; ADP, adenosine 5′-diphosphate; PP, inorganic pyrophosphate; P_i, orthophosphate; PPase, pyrophosphatase; HPLC, high-performance liquid chromatography; CD, circular dichroic; NMR, nuclear magnetic resonance; MES, 2-(*N*-morpholino)ethanesulfonate; NADP, nicotinamide adenine dinucleotide phosphate; NTP, nucleoside triphosphate; PEP, phosphoenolpyruvate; glucose-6-P dehydrogenase, glucose-6-phosphate dehydrogenase.

0006-2960/87/0426-2060$01.50/0

the preparation and characterization of exchange-inert Rh(III)–polyphosphate complexes (Lin et al., 1984a). In this paper we examine (i) the structure of the P^1,P^2-bidentate $Rh(H_2O)_4PP$ (**1**) ring system, which is the basic structural unit of the $Rh(H_2O)_n$-polyphosphate complex, (ii) the substrate activity of P^1,P^2-bidentate $Rh(H_2O)_4PP$ with yeast inorganic pyrophosphatase, and (iii) the binding affinities of the two α,β-bidentate $Rh(H_2O)_4ADP$ (**2**) stereoisomers (Δ and Λ) for selected kinases.

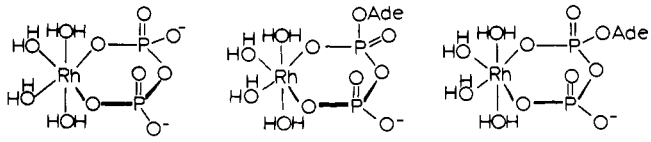

1 2 Δ 2 Λ

Materials and Methods

Materials

PPase was purified according to the modified (Bond, 1979) method of Cooperman et al. (1973). The enzyme used in these experiments migrated as a single band on sodium dodecyl sulfate–polyacrylamide gel electrophoresis gels (7.5% acrylamide) and had an activity of 690 μmol of P_i min^{-1} (mg of protein)$^{-1}$ at pH 7.5. All other enzymes used as well as the buffers, substrates, and cofactors were purchased from Sigma Chemical Co. The 99% ^{18}O-enriched water was purchased from Cambridge Isotopes Co. P^1,P^2-Bidentate $Rh(H_2O)_4PP$ and α,β-bidentate $Rh(H_2O)_4ADP$ were prepared according to the method of Lin et al. (1984a). [^{32}P]PP was purchased from Amersham.

Methods

$[Rh(H_2O)_4H_2P_2O_7]^+Cl^-$ (M_r 386.4) Crystal Structure. Crystals suitable for X-ray analysis were grown at 4 °C from concentrated $Rh(H_2O)_4PP$ solutions (Lin et al., 1984a) that were 10 mM in HCl (pH ~2) and 5% in MeOH. The complex crystallizes in the orthorhombic space $P2_12_12_1$ ($Z = 4$) with cell constants $a = 5.947$ (2) Å, $b = 12.462$ (2) Å, and $c = 12.902$ (2) Å. X-ray data were collected on an Enraf-Nonius CAD4 diffractometer using Mo Kα radiation (λ = 0.7107 Å). Out of 3339 unique reflections measured up to a 2θ limit of 80°, 2875 with $I/[\sigma(I)] > 2$ were considered observed and used for the structure analysis. The data were corrected for Lorentz, polarization, and absorption effects. No significant crystal decay was observed during data collection. The structure was solved by the heavy-atom technique, and the nonhydrogen atoms were refined by the least-squares method, using anisotropic temperature factors and a counting statistics weighting scheme with the weights proportional to $1/[\sigma^2F + (0.01F_0)^2]$.

All of the hydrogen atoms were located from difference Fourier syntheses, although a few were barely discrenible from background. The weaker proton densities were confirmed and distinguished from noise-density peaks by checking their geometry relative to other atoms, including potential hydrogen bond acceptors. The hydrogen atoms were assigned a fixed temperature factor of 4.0 Å^2 and were not refined. The non-hydrogen atoms were subsequently refined to convergence. The hydrogen atom scattering was included in the structure factor calculation to a final R index of 0.031 and a maximum shift/error ratio of 0.01 in the final cycle of refinement.

$Rh(H_2O)_4PP$/Pyrophosphatase Reactions. [^{32}P]$Rh(H_2O)_4PP$ was prepared from [^{32}P]PP and $Rh(H_2O)_6^{3+}$ according to the method of Lin et al. (1984a). The reactions (0.5-mL volume, 23 °C) were buffered at pH 6.0 by 75 mM K^+-MES. Each contained 30 mM Cl^- and varying amounts of Mg^{2+} and [^{32}P]$Rh(H_2O)_4PP$. Reactions were initiated by the addition of pyrophosphatase, allowed to proceed to 10–15% conversion, and then terminated by the addition of 100 μL of 6 N HCl. The reaction mixture was then treated with EDTA and assayed for [^{32}P]P_i (Knight et al., 1981). The velocity of the pyrophosphatase-catalyzed hydrolysis of $Rh(H_2O)_4PP$ was measured at six different concentrations of the complex (at levels $^1/_2$–5 times K_m) and at six different Mg^2 concentrations (at levels $^1/_2$–5 times K_m). The V_m, K_{iA}, and K_B values were calculated by using

$$V_0 = V_mAB/(K_BA + AB + K_{iA}K_B) \quad (1)$$

where K_{iA} = dissociation constant of EA, K_B = Michaelis constant of B, A and B = substrate concentrations, V_0 = initial velocity, and V_m = maximal velocity.

Stereochemical Assignment of $Rh(H_2O)_4ADP$. (R_P)-[α-^{16}O,^{18}O]ADP was prepared according to the method described by Speckhard et al. (1986). The ratio of the ^{18}O-labeled species to the all ^{16}O-labeled species was determined by ^{31}P NMR techniques to be ca. 9:1. The (R_P)-[α-^{16}O,^{18}O]$Rh(H_2O)_4ADP$ complex was prepared from an equal mixture of (R_P)-[α-^{16}O,^{18}O]ADP and [α-^{16}O]ADP according to the method of Lin et al. (1984a). The complex was purified by using Dowex-50 (H^+) column chromatography and then resolved into the Λ and Δ screw sense isomers by using preparative reverse-phase HPLC [10 mM methanesulfonic acid (pH 2.2)] (Lin et al., 1984a). The ^{31}P NMR samples of the two screw sense isomers at pH 3 contained ca. 0.1 M methanesulfonic acid, 50% D_2O, and 2 mM CDTA. Proton spin decoupled ^{31}P NMR spectra were recorded at 20 °C by using a Bruker Model AM-400 NMR spectrometer operating at 161 MHz. We found that, for $Rh(H_2O)_4ADP$ isomer 1 (Λ), Pα (doublet) was 3.453 ± 0.003 ppm and Pβ (doublet) was 8.401 ± 0.003 ppm ($J_{\alpha,\beta}$ = 20.7 Hz). The ^{18}O isotopic shift at Pα was 0.015 ppm. For $Rh(H_2O)_4ADP$ isomer 2 (Δ), Pα (doublet) was 3.556 ± 0.003 ppm and Pβ (doublet) was 8.478 ± 0.003 ppm ($J_{\alpha,\beta}$ = 20.6 Hz). The ^{18}O isotopic shift at Pα was 0.025 ppm. The chemical shifts were referenced to H_3PO_4, the external reference.

Determination of the Λ and Δ $Rh(H_2O)_4ADP$ Inhibition Constants. The kinase inhibition studies were carried out at 25 °C and pH 6.0. All reactions contained 50 mM K^+-MES and 10 mM $MgCl_2$. The glucose-6-P dehydrogenase (10 units/mL)/NADP (1 mM) couple was used to monitor the hexokinase-catalyzed reaction of glucose (10 mM) and MgATP (30–300 μM). The hexokinase/glucose-6-P dehydrogenase couple (50 units/mL hexokinase, 10 units/mL glucose-6-P dehydrogenase, 10 mM glucose, and 1 mM NADP) was used to monitor the creatine kinase catalyzed reaction of creatine phosphate (10 mM) and MgADP (30–500 μM), the arginine kinase catalyzed reaction of arginine phosphate (10 mM) and MgADP (0.1–2.0 mM), and the acetate kinase catalyzed reaction of acetyl phosphate (2 mM) and MgADP (60–600 μM). The lactate dehydrogenase (10 units/mL)/NADH (0.4 mM) coupled assay was used to monitor the pyruvate kinase catalyzed reaction of PEP (5 mM) and MgADP (50–500 μM), and the pyruvate kinase (50 units/mL)/lactate dehydrogenase (10 units/mL)/PEP (5 mM)/NADH (0.4 mM) coupled assay was used to monitor the glycerokinase-catalyzed reaction of glycerol (1.0 mM) and MgATP (30–250 μM). The K_i values were calculated from the initial velocity data by using the equation $V_0 = V_mA/[K_m(1 + I/K_i) + A]$, where V_0 = initial velocity, V_m = maximum velocity, K_m = Michaelis constant, K_i = inhibition constant, and I = inhibitor concentration.

Table I: Fractional Positional Parameters for All Atoms of RhPP[a]

atom	X	Y	Z	B_{eq} or B
Rh	37785 (5)	56034 (2)	17337 (2)	1.01 (0)
P(1)	56330 (17)	44460 (7)	36810 (6)	1.07 (1)
P(2)	63353 (18)	67294 (7)	35009 (7)	1.15 (1)
O1(P1)	56979 (52)	45261 (21)	24949 (19)	1.43 (4)
O2(P1)	73604 (62)	36763 (20)	40763 (22)	1.77 (6)
O3(P1)	32574 (56)	42688 (22)	40716 (23)	1.75 (5)
O(P12)	64083 (57)	56050 (18)	41276 (20)	1.67 (5)
O1(P2)	41614 (51)	67040 (20)	28445 (20)	1.44 (5)
O2(P2)	84369 (53)	67733 (28)	28441 (26)	2.20 (6)
O3(P2)	61286 (76)	75648 (20)	43384 (22)	2.18 (7)
OW(1)	18232 (57)	66460 (21)	9354 (21)	1.66 (5)
OW(2)	32116 (99)	45085 (24)	6035 (27)	3.82 (12)
OW(3)	66299 (69)	60992 (37)	10352 (23)	3.25 (9)
OW(4)	9667 (54)	50766 (22)	24652 (24)	1.72 (5)
Cl	113801 (18)	83266 (7)	36767 (7)	1.67 (2)
H(O3P1)	202 (5)	463 (14)	363 (6)	4.0
H(O2P2)	961 (5)	725 (16)	310 (5)	4.0
H1(W1)	235 (5)	723 (16)	98 (5)	4.0
H2(W1)	179 (5)	649 (16)	30 (5)	4.0
H1(W2)	296 (5)	474 (15)	1 (6)	4.0
H2(W2)	398 (5)	389 (16)	64 (6)	4.0
H1(W3)	730 (6)	665 (15)	146 (6)	4.0
H2(W3)	651 (5)	634 (16)	42 (5)	4.0
H1(W4)	11 (5)	566 (16)	252 (7)	4.0
H1(W4)	44 (5)	445 (16)	207 (6)	4.0

[a] Values are multiplied by 10^5 for non-hydrogen atoms and 10^3 for hydrogen atoms.

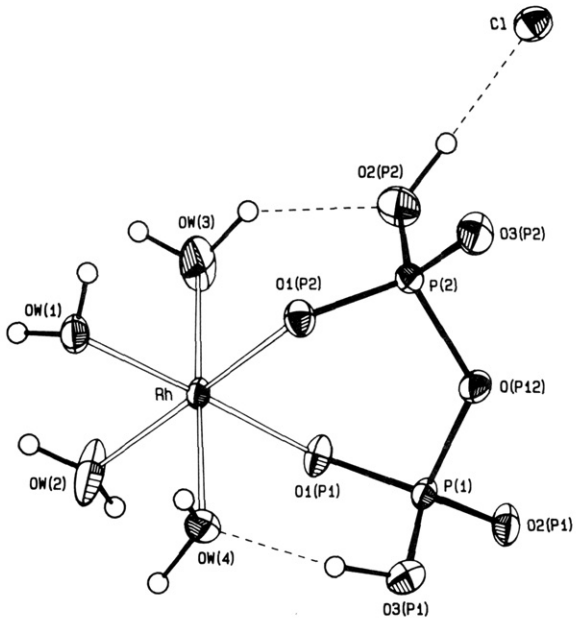

FIGURE 1: ORTEP drawing of the rhodium(III)–pyrophosphate complex showing non-hydrogen atoms as 50% thermal probability ellipsoids and hydrogen atoms as spheres of arbitrary size.

RESULTS

Crystal Structure of $[Rh(H_2O)_4H_2P_2O_7]^+Cl^-$. Atomic coordinates are given in Table I, and an ORTEP drawing (Johnson, 1976) of the structure is presented in Figure 1. Bond lengths and chelate ring bond angles are given in Figure 2. Hydrogen bonds are listed in Table III and depicted in Figure 3. The chelate ring conformation, metal–oxygen bond distances, and hydrogen bonds of the $Rh(H_2O)_4PP$ structure are compared below with the corresponding $Cr^{III}PP$ and $Co^{III}PP$ complexes (Merritt & Sundaralingam, 1980; Merritt et al., 1981; Haromy et al., 1984).

Chelate Ring Conformation. The conformations of the metal–O1(P1)–P(1)–O(P12)–P(2)–O1(P2) ring of $Rh(H_2O)_4PP$ (see Figure 1) and the corresponding $Cr^{III}PP$ and

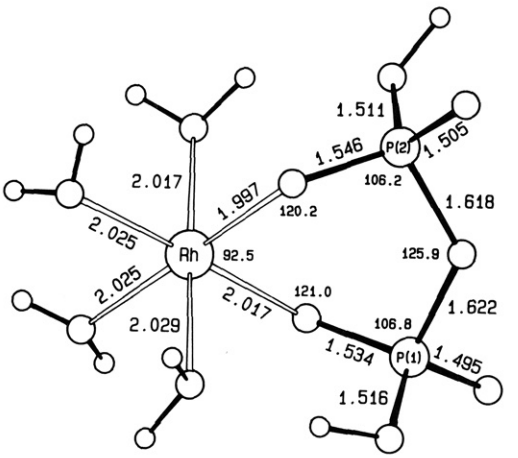

FIGURE 2: Non-hydrogen atom bond distances and chelate ring bond angles for the RhPP complex. The estimated standard deviations are 0.003 Å for bond lengths and 0.2° for bond angles.

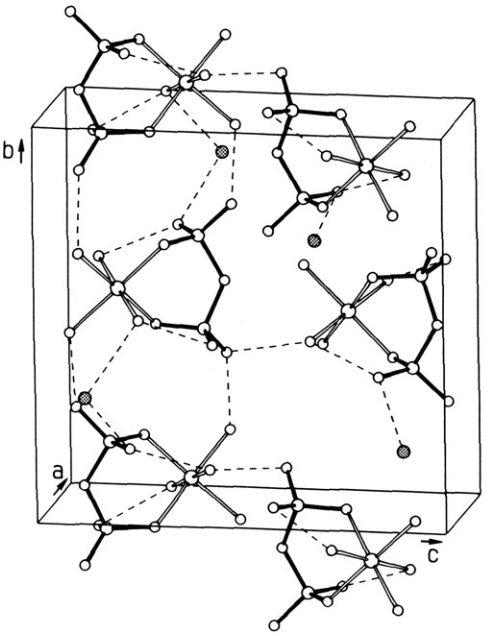

FIGURE 3: Packing diagram of the RhPP complex. The chloride ions are shaded, and hydrogen bonds are indicated with dashed lines.

Table II: Conformation of the Metal-O1(P1)–O(P12)–P(1)–P(2)–O1(P2) Ring for Rhodium Pyrophosphate and Some Related Complexes

complex	Q (Å)	θ (deg)	φ (deg)
$Rh(H_2O)_4PP$	0.756 (3)	88.7 (3)	263.5 (2)
$Cr(H_2O)_4PP$[a]	0.575	96.2	306.7
$Cr(NH_3)_4PP$[b]	0.618	88.8	104.3
$Co(NH_3)_4PP$[c]	0.623	86.8	107.6

[a] Values are taken from Merritt et al. (1981). [b] Values are taken from Haromy et al. (1984). [c] Values are taken from Merritt and Sundaralingam (1980).

$Co^{III}PP$ complexes (Merritt & Sundaralingam 1980; Merritt et al., 1981; Haromy et al., 1984) are summarized in Table II. The ring-puckering amplitude is measured by Q, the chair to boat transition is defined by θ (0° or 180° = chair, 90° = boat), and the boat to twist-boat interconversion is given by the pseudorotation angle ϕ (0° = boat, 30° = twist-boat, 60° = boat, 90° = twist-boat, etc.). The tetraaqua–RhPP complex, which assumes the twist-boat conformation, exhibits the largest puckering (Q) of the structures investigated (Table II). The tetraaqua–CrPP complex, which is found in the boat conformation, displays a somewhat flatter ring (smaller Q). The

Table III: List of Hydrogen Bonds for the RhPP Complex

A–H···B	sym[a] code	translation			distances (Å)			A–H···B (deg)
		x	y	z	A–H	H···B	A···B	
O3(P1)–H(O3P1)···OW(4)	1	0	0	0	1.03	1.72	2.677	152
O2(P2)–H(O2P2)···Cl	1	0	0	0	0.97	1.86	2.822	169
OW(1)–H1(W1)···O2(P1)	4	1	0	0	0.79	1.81	2.576	161
OW(1)–H2(W1)···O3(P1)	2	0	1	−1	0.84	1.85	2.662	163
OW(2)–H1(W2)···O3(P1)	2	0	1	−1	0.83	1.88	2.644	153
OW(2)–H2(W2)···O3(P2)	4	1	−1	0	0.90	1.65	2.455	147
OW(3)–H1(W3)···O2(P2)	1	0	0	0	0.96	1.92	2.703	137
OW(3)–H2(W3)···O2(P1)	2	1	1	−1	0.85	1.86	2.613	147
OW(4)–H1(W4)···O2(P2)	1	−1	0	0	0.89	1.76	2.641	171
OW(4)–H2(W4)···Cl	4	1	−1	0	0.98	2.01	2.979	166

[a] Symmetry codes: (1) x, y, z; (2) $^1/_2 - x, -y, ^1/_2 + z$; (3) $^1/_2 + x, ^1/_2 - y, -z$; (4) $-x, ^1/_2 + y, ^1/_2 - z$.

isomorphous tetraammine–Co(III) (Merritt & Sundaralingam, 1980) and –Cr(III) (Haromy et al., 1984) complexes assume boat/twist-boat conformations with an intermediate degree of ring puckering (Q value).

Metal–Oxygen Bond Distances. The Rh–O coordination distances of $Rh(H_2O)_4PP$ (Figure 2) are significantly longer [average of 2.02 (1) Å for all six bonds] than the corresponding Cr–O distances [1.96 (2) Å] for the tetraaqua–Cr complex (Merritt et al., 1981). Similarly, the metal to bridge oxygen atom distance of 3.462 (3) Å is significantly longer than that for the corresponding Cr complex [3.405 (3) Å]. In both structures the two metal–pyrophosphate coordination distances are asymmetric, with a difference of 0.02 Å for the Rh structure [2.017 (3) vs. 1.997 (3) Å] and a slightly greater difference for the Cr structure [1.935 (3) vs. 1.966 (3) Å]. In contrast, the tetraammine–Co and –Cr structures have symmetric coordination bond lengths, with a difference <0.01 Å. Unlike the Cr and Co complexes, where the P–O bonds involving the bridge oxygen atom are significantly asymmetric (differing by >0.03 Å), the corresponding bonds of the Rh complex are of virtually equal length. The chelate ring angle at the Rh atom is 92.5°. The angles of the coordinated oxygen atom (120.2° and 121.0°) are substantially smaller than the corresponding angles for the tetraaqua–Cr complex (125.9° and 132.7°) or the tetraammine–Cr complex (127.5° and 128.3°). These narrow angles result from the lengthening of the coordination bond lengths and the elongation of one of the P–O1 bonds from an average of 1.517 (3) to 1.546 (3) Å.

Hydrogen Bonding. All 10 protons of the Rh(III)PP complex participate in hydrogen bonding (Table III and Figure 3). Two of these are intramolecular hydrogen bonds between the phosphate oxygen atoms and the axially coordinated water molecules (Figure 1). OW(4) accepts a proton from O3(P1) [with a oxygen to oxygen distance of 2.677 (4) Å] while OW(3) donates a proton to O2(P2) with a slightly longer distance of 2.703 (4) Å. A packing diagram of the RhPP complex is shown in Figure 3. There are six hydrogen bonds between symmetry-related tetraaqua(pyrophosphato)rhodium(III) complexes [with distances ranging from 2.455 (4) to 2.662 (4) Å] and two hydrogen bonds to the chloride ion [with distances of 2.822 (3) and 2.979 (3) Å]. In contrast to the present structure, the tetraaqua–Cr structure exhibits no intramolecular hydrogen bonds. The tetraammine–Co and –Cr structures exhibit two intramolecular hydrogen bonds from the two axial ammine ligands to the phosphate oxygen atoms.

Pyrophosphatase-Catalyzed Hydrolysis of $Rh(H_2O)_4PP$. Yeast inorganic pyrophosphatase catalyzes the hydrolysis of P^1,P^2-bidentate $Cr(H_2O)_4PP$, $Cr(NH_3)_4PP$, and $Co(NH_3)_4PP$ complexes (Knight et al., 1981, 1983). Two Mg(II) ions per active site are required for catalytic hydrolysis of these complexes (Knight et al., 1984). One Mg(II) ion binds to the enzyme so tightly that, under the reaction conditions of high cofactor/enzyme, the high-affinity binding site is filled. The second Mg(II) ion binds in rapid equilibrium after the metal–PP complex is bound. Thus, in order to evaluate the kinetic constants of the $Rh(H_2O)_4PP$ complex as a substrate for pyrophosphatase, the reaction velocity was measured as a function of the concentrations of $Rh(H_2O)_4PP$ and Mg(II). The data obtained were analyzed by using an initial velocity equation describing a rapid equilibrium ordered bi bi kinetic mechanism. The kinetic constants of the $Rh(H_2O)_4PP$/Mg(II)/pyrophosphatase reaction are shown in Table IV along with those measured for the corresponding $Cr^{III}PP$ and $Co^{III}PP$ complexes (Knight et al., 1981, 1983; Haromy et al., 1982). Also shown in Table IV are the K_m values and turnover numbers reported for MgPP and for a representative[2] lanthanide $M^{III}PP$ complex (Ting & Dunaway-Mariano, 1984). The data shown in Table IV demonstrate the following: (i) the lanthanide $M^{III}PP$ complexes and $Mg^{II}PP$ complex display comparable substrate activities, (ii) the tetraaqua exchange-inert complexes display K_i values that are comparable to the K_m values obtained for $Mg^{II}PP$ or lanthanide $M^{III}PP$ complexes and turnover numbers that are considerably smaller, (iii) the exchange-inert tetraaqua complexes [$Rh(H_2O)_4PP$ and $Cr(H_2O)_4PP$] have kinetic constants of comparable value as do the tetraammine complexes [$Cr(NH_3)_4PP$ and $Co(NH_3)_4PP$], and (iv) the binding affinities and turnover numbers of the exchange-inert tetraammine complexes are significantly smaller than those of the corresponding tetraaqua complexes.

Table IV: Kinetic Constants for the Pyrophosphatase/Metal–PP/Mg^{2+} Reaction (pH 6.3, 23 °C)

complex	K_{iA} (mM)	V_m (min^{-1})	K_m (Mg^{2+}) (mM)
$Rh(H_2O)_4PP$	0.063 ± 0.007	500 ± 100	1.9 ± 0.2
$Cr(H_2O)_4PP$[a]	0.068 ± 0.008	320 ± 90	1.3 ± 0.4
$Cr(NH_3)_4PP$[a]	0.48 ± 0.06	15 ± 2	0.43 ± .07
$Co(NH_3)_4PP$[a]	1.8 ± 0.3	7.5 ± 0.8	0.5 ± 0.1
MgPP[b]	0.020 ± 0.002	1×10^4	
LuPP[b,c]	0.21 ± 0.02	1×10^4	

[a] These values were taken from Knight et al. (1984). [b] These K_m and V_m values were measured in the presence of saturating Mg^{2+}. [c] These values were taken from Ting and Dunaway-Mariano (1984).

Stereochemical Assignment of the Λ and Δ α,β-Bidentate $Rh(H_2O)_4ADP$ Screw Sense Isomers. For the purpose of determining the configuration at α-P of the two $Rh(H_2O)_4ADP$ screw sense isomers, (R_P)-[α-^{16}O,^{18}O]ADP

[2] The V_m values for a number of lanthanide–PP complexes are equivalent to the V_m of MgPP [see Ting and Dunaway-Mariano (1984)]. LuPP is used as an example in Table IV.

Table V: Inhibition Constants of α,β-Bidentate $Rh(H_2O)_4ADP$ and $Cr(H_2O)_4ADP$ Isomers as Competitive Inhibitors vs. MgADP of Several Kinases

enzyme	$Rh(H_2O)_4ADP$ (mM)		$Cr(H_2O)_4ADP$ (mM)[a]	
	Δ isomer	Λ isomer	Δ isomer	Λ isomer
pyruvate kinase	1.3 ± 0.2	0.65 ± 0.06	3.8 ± 0.4	1.16 ± 0.06
acetate kinase	0.04 ± 0.01	0.025 ± 0.007	0.068 ± 0.008	0.061 ± 0.006
hexokinase[b]	1.5 ± 0.1	0.77 ± 0.02	1.8 ± 0.08	2.1 ± 0.1
glycerokinase[b]	0.17 ± 0.03	0.6 ± 0.1		
myokinase			1.3 ± 0.1	0.92 ± 0.07
creatine kinase	0.0038 ± 0.0005	0.17 ± 0.03	0.0073 ± 0.0003	0.15 ± 0.01
arginine kinase	0.06 ± 0.01	0.4 ± 0.1		

[a] Values were taken from Dunaway-Mariano and Cleland (1980). [b] Vs. MgATP.

(Sammons & Frey, 1982) was prepared according to the method of Speckhard et al. (1986). After the chiral ^{18}O-labeled ADP was mixed with an equal quantity of [α-^{16}O]ADP, it was reacted with $Rh(H_2O)_6^{3+}$ to generate $Rh(H_2O)_4$[α-^{16}O]ADP and $Rh(H_2O)_4$[α-^{16}O,^{18}O]ADP in a 1:1 ratio as a mixture of stereoisomers. The Λ and Δ screw sense isomers were separated by using reverse-phase HPLC techniques. The ^{31}P NMR spectra of each screw sense isomer showed two doublets for the α-P resonance. In the case of the first isomer to elute from the HPLC column (designated isomer 1), the chemical shift difference between the α-P resonances is 0.015 ppm, while in the case of the second isomer to elute from the column (designated isomer 2), the shift difference is 0.025 ppm. On the basis of previous studies of the ^{18}O-induced chemical shifts of α-P resonances due to Co(III) coordination of dADP (Coderre & Gerlt, 1980), ADP (Sammons & Frey, 1982), and ATP (Speckhard et al., 1986), $Rh(H_2O)_4ADP$ isomer 1 is assigned the Λ configuration and isomer 2 is assigned the Δ configuration.

Stereospecificity of Kinases in Binding α,β-Bidentate $Rh(H_2O)_4ADP$ Screw Sense Isomers. The binding affinities of the Λ and Δ $Rh(H_2O)_4ADP$ screw sense isomers toward hexokinase, glycerokinase, creatine kinase, arginine kinase, pyruvate kinase, and acetate kinase were examined by testing these complexes as inhibitors vs. MgATP or MgADP. In each instance competitive inhibition was observed. In Table V the K_i values obtained for the $Rh(H_2O)_4ADP$ screw sense isomers are recorded along with those obtained for the $Cr(H_2O)_4ADP$ screw sense isomers (Dunaway-Mariano & Cleland, 1980). In general, the $Rh(H_2O)_4ADP$ isomers were found to bind to the kinases with approximately the same affinity as the $Cr(H_2O)_4ADP$ isomers.

Discussion

Owing to the chelate effect Mg(II) will coordinate to more than one oxygen atom of the polyphosphate ligand to form either one or two chelate rings. In most chemical and biochemical reactions of the Mg(II)–polyphosphate complex, the chelate ring constitutes the "business end" of the molecule. Consequently, the electronic and structural features of this chelate ring strongly influence the reactivity of the metal–polyphosphate complex under a given set of conditions.

The work reported in this paper is part of a larger effort to develop exchange-inert metal–polyphosphate complexes as probes of the structures and dynamics of Mg(II)–polyphosphate complexes in solution and in the binding sites of proteins. The results emanating from this effort suggest that Rh(III)–polyphosphate complexes are superior to the analogous Cr(III) and Co(III) complexes as models of Mg(II)–polyphosphate complexes. Specifically, the Rh(III) complexes display the desirable biochemical properties of the aqua–Cr(III)–polyphosphate models, and at the same time they are both easily prepared and easily characterized. Moreover, the electronic and structural differences that we have found existing between the six-membered chelate rings of the Rh(III), Cr(III), and Co(III) complexes provide the necessary data base for future structure/activity studies.

Substrate Activity of P^1,P^2-Bidentate $Rh(H_2O)_4PP$. The use of Rh(III) as a model for Mg(II) in biochemical processes was first examined by testing the substrate activity of P^1,P^2-bidentate $Rh(H_2O)_4PP$ with yeast inorganic pyrophosphatase (see Table IV). The $Rh(H_2O)_4PP$ and $Cr(H_2O)_4PP$ complexes show comparable substrate activities that are approximately 2 orders of magnitude greater than those of the two tetraammine complexes, $Cr(NH_3)_4PP$ and $Co(NH_3)_4PP$. The high K_m and low V_m values of the tetraammine complexes underscore the necessity of choosing *aqua*–metal polyphosphates as biochemical models of Mg(II)–polyphosphates.

In order to access the significance of the contrastingly similar kinetic properties yet different structural and electronic properties observed for the $Rh(H_2O)_4PP$ and $Cr(H_2O)_4PP$ complexes, the comparative substrate activities of the lanthanide–PP complexes (Ting & Dunaway-Mariano, 1984) and MgPP must be taken into account. First, the V_m values obtained for the pyrophosphatase-catalyzed hydrolysis of $Cr(H_2O)_4PP$ and $Rh(H_2O)_4PP$ are considerably smaller than those found for MgPP (Table IV). The earlier studies of Knight et al. (1981) showed that $Mg(H_2O)_4PP$ in its fully ionized form (net charge of −2) is the substrate of this enzyme. Thus, the slow turnover of the $Cr(H_2O)_4PP$ and $Rh(H_2O)_4PP$ complexes might be a result of the fact that under the reaction conditions they possess a net charge of −1. However, recent studies (Ting & Dunaway-Mariano, 1984) have shown that a number of lanthanide–PP complexes [$(LuPP)^{1-}$, for example, Table IV] have the same turnover rate as $(MgPP)^{2-}$. Hence, the degree of protonation rather than net charge of the complex appears to determine reactivity. The disparity in the V_m values observed for the lanthanide–PP and $Cr(H_2O)_4PP$/$Rh(H_2O)_4PP$ complexes is probably due to the inertness of the Cr(III) and Rh(III) centers toward ligand exchange. Although the resistance of the Cr(III) and Rh(III) complexes to undergo ligand exchange could interfere with productive binding, its most profound effect will be exerted through interruption of the normal course of catalysis. Specifically, once the $Mg(H_2O)_4PP$ complex is hydrolyzed to the *cis*-$Mg(H_2O)_4(P_i)_2$ complex, further hydrolysis must take place at the metal center prior to product release. Being a reaction intermediate, $Mg(H_2O)_4(P_i)_2$ is not released from the enzyme during catalysis (Haromy et al., 1982). In the case of hydrolysis of the Cr(III) and Rh(III) complexes, exchange-inert $M^{III}(H_2O)_4(P_i)_2$ complexes are formed that must be released directly from the enzyme before another catalytic cycle can begin. Since the exchange-inert $M^{III}(H_2O)_4(P_i)_2$ complexes are stable analogues of the reaction intermediate, their release from the enzyme will be slow (Haromy et al., 1982; Duna-

Scheme I

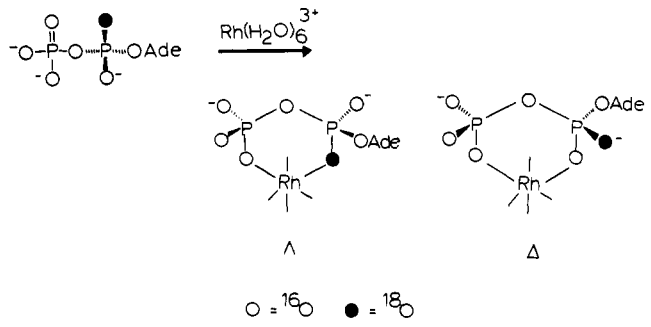

way-Mariano & Cleland, 1980). Moreover, if $M^{III}(H_2O)_4(P_i)_2$ is released significantly more slowly than it is formed, a small perturbation in the hydrolysis rate caused by structural differences between the Cr(III) and Rh(III) complexes would not influence the turnover rates of these complexes. Thus, the similar V_m values observed with the $Cr(H_2O)_4PP$ and $Rh(H_2O)_4PP$ complexes may be a reflection of rate-limiting product release rather than of their equivalent reactivity.

Properties of the Λ and Δ α,β-Bidentate $Rh(H_2O)_4ADP$ Isomers: Configuration Assignment. The first task at hand was to assign the α-P configuration of the two $Rh(H_2O)_4ADP$ diastereomers. This was accomplished by using an NMR-based approach wherein the two $Rh(H_2O)_4ADP$ screw sense isomers were prepared from (R_P)-[α-^{16}O,^{18}O]ADP (see Scheme I) and separated and the ^{18}O-induced chemical shift of the α-P resonance of each isomer was measured. Corderre and Gerlt (1980) had previously shown with the analogous system α,β-bidentate $Co(NH_3)_4$[α-^{16}O,^{18}O]dADP that metal coordination to the α-^{18}O atoms rather than the α-^{16}O atoms of the phosphoryl residue reduced the α-P chemical shift from ca. 0.030 ppm to ca. 0.017 ppm. We found similar results for Rh(III) coordination to the α-^{18}O vs. α-^{16}O of the (R_P)-[^{16}O,^{18}O]ADP. Thus, these results allowed us to make the configurational assignments to the $Rh(H_2O)_4ADP$ screw sense isomers as outlined in Scheme I.[3]

Unlike the case of the $Rh(H_2O)_4ADP$ and $Co(NH_3)_4ADP$ complexes, the configurations of the screw sense isomers of $Cr(H_2O)_4ADP$ and $Cr(NH_3)_4ADP$ cannot be assigned by using the NMR-based approach. However, by comparison of the physical and biochemical properties of the screw sense isomers of $Cr^{III}ADP$ with those of the analogous Co(III) and Rh(III) complexes, configurational assignment can be made with a reasonable degree of accuracy. For example, the Λ screw sense isomers of $Rh(H_2O)_4ADP$, $Co(NH_3)_4ADP$, $Cr(H_2O)_4ADP\alpha S$, $Cr(NH_3)_4ADP\alpha S$, and $Co(NH_3)_4ADP\alpha S$ all have shorter retention times on reverse-phase HPLC (Lin et al., 1984b) than do their Δ isomers. In addition, the Λ screw isomers of these complexes display CD spectra characterized by a positive Cotton effect at λ_{max} [ca. 550 nm for the Co(III) and Cr(III) complexes and ca. 400 nm for the Rh(III) complex] while the Δ screw sense isomers display CD spectra characterized by a negative Cotton effect at λ_{max}. The $Cr(H_2O)_4ADP$ and $Cr(NH_3)_4ADP$ screw sense isomers having the shortest retention times on reverse-phase HPLC also yield CD spectra that are characterized by a positive Cotton effect at λ_{max} (Lin et al., 1984b). The chromatographic and optical properties of these screw sense isomers are consistent with a Λ configuration.[4] Likewise, the $Cr^{III}ADP$ screw sense isomers having the longest retention time on HPLC show a negative Cotton effect at λ_{max}, and these are assigned the Δ configuration.

The respective screw sense isomers of the $Cr^{III}ADP$, $Co^{III}ADP$, and $Rh^{III}ADP$ complexes also display distinct binding affinities toward creatine kinase, which supports the $Cr^{III}ADP$ configurational assignment. Specifically, the Δ isomers of $Co(NH_3)_4ADP$ (Dunaway-Mariano & Cleland, 1980) and $Rh(H_2O)_4ADP$ (see Table V) and (what we presumed to be) the Δ isomers of $Cr(H_2O)_4ADP$ and $Cr(NH_3)_4ADP$ (Dunaway-Mariano & Cleland, 1980) all bind to the MgADP binding site of creatine kinase significantly tighter than do the corresponding Λ isomers.

Kinase Specificity. Previous studies of kinases (Dunaway-Mariano & Cleland, 1980) have shown that exchange-inert metal–ADP complexes cannot substitute for MgADP as substrates because of the necessity for insertion of the phosphoryl group of the cosubstrate into the coordination sphere of the metal during the course of catalysis. Thus, our evaluation of the $Rh(H_2O)_4ADP$ complex as a $Mg(H_2O)_4ADP$ model in kinase-catalyzed reactions relied on an evaluation of the ability of the $Rh(H_2O)_4ADP$ to compete with MgADP for the kinase substrate binding site. The inhibition constants obtained for the two $Rh(H_2O)_4ADP$ screw sense isomers are presented in Table V along with those reported previously for the $Cr(H_2O)_4ADP$ screw sense isomers (Dunaway-Mariano & Cleland, 1980). For most of the kinase reactions studied, the K_i values obtained for the $Rh(H_2O)_4ADP$ isomers agree well with those obtained previously for the $Cr(H_2O)_4ADP$ isomers. Moreover, the dissociation constants for the kinase–$Rh(H_2O)_4ADP$ and kinase–$Cr(H_2O)_4ADP$ complexes are remarkably similar to those reported for the corresponding kinase–MgADP complexes (Rao et al., 1976, 1978; Janson & Cleland, 1974; Viola et al., 1982; Schimerlik & Cleland, 1973).

A second observation worth noting is that both creatine kinase and arginine kinase bind the $Rh(H_2O)_4ADP$ Δ screw sense isomers much more tightly than the $Rh(H_2O)_4ADP$ Λ screw sense isomers. Previous studies of the substrate specificity of these enzymes using the thionucleotide approach[5] have shown that the active MgADP complex is α,β-bidentate and that the Δ isomer, rather than the Λ isomer, is recognized as substrate by these enzymes (Burgers & Eckstein, 1980; Cohn et al., 1982). Thus, the stereospecificity displayed by creatine kinase and arginine kinase in binding the Δ $Rh(H_2O)_4ADP$ isomer reflects the steric constraints of the α,β-bidentate MgADP binding sites on these enzymes. Related thionucleotide-based studies of the MgATP/MgADP substrate structure for the enzymes hexokinase (Jaffe & Cohn, 1979), myokinase (Tomasselli & Noda, 1983), and acetate kinase (Romaniuk & Eckstein, 1981) indicate that the β-monodentate MgADP complex is the active species. Since the α,β-bidentate chelate structure is not found in the actual substrate, it is not surprising to find that these enzymes show no discrimination in binding the $Cr(H_2O)_4ADP$ or $Rh(H_2O)_4ADP$ screw sense

[3] The perturbation of the isotopic shift results from a decrease in the P–^{18}O π bond order when the metal ion is coordinated to the heavy oxygen atom relative to when it is not. The decrease in P–O π bond order upon metal coordination is reflected by the greater P–O bond length for the metal-coordinated oxygen atom than for an oxygen atom bonded to phosphorus alone. The increase in P–O bond length upon Co(III) coordination is similar to the increase observed upon Rh(III) coordination, as evidenced by the X-ray structures of $Co(NH_3)_4PP$ (Merritt & Sundaralingam, 1980) and $Rh(H_2O)_4PP$ (this study).

[4] We do not mean to imply that the relationship between Cotton effect and screw sense observed for one coordination complex should necessarily hold for a different complex. We are simply noting a trend.

[5] According to this method Mg^{2+} and Cd^{2+} complexes of individual ATPβS and ATPαS (or ADPαS) diastereomers are tested as substrates for the kinase [see Eckstein (1985)].

isomers (Table V). In fact, in the case of hexokinase the very weak binding observed for bidentate $Rh(H_2O)_4ADP$ and $Cr(H_2O)_4ADP$ is consistent with the weak binding observed for MgADP (which is primarily bidentate) (K_D = 1.6 mM; Viola et al., 1982) and the tight binding observed for β-monodentate $Cr(H_2O)_5ADP$ (K_i = 0.003 mM; Dunaway-Mariano & Cleland, 1980).

$Rh(H_2O)_4PP$ Chelate Ring Structure. A comparison of the crystal structures of $Rh(H_2O)_4PP$, $Cr(H_2O)_4PP$, $Cr(NH_3)_4PP$, and $Co(NH_3)_4PP$ (see Results) reveals that distinct differences exist between their H-bonding patterns (both intramolecular H bonds and intermolecular H bonds) and chelate ring conformations. Subtle, yet significant, differences also exist between these complexes with respect to their M–O and P–O bond lengths and chelate ring bond angles viz., O–M–O and P–O–P).

To the extent that the structural differences existing between the $Cr^{III}PP$ and $Rh^{III}PP$ complexes may also exist between the $Cr^{III}ADP$ and $Rh^{III}ADP$ complexes, they do not affect the binding affinities of the latter complexes toward kinases. Because binding affinity alone is not expected to be very sensitive to such subtle structural or electronic differences in the metal–ADP complexes, this finding is to be expected. On the other hand, the rate of a catalyzed phosphoryl transfer from the chelate ring of the metal–PP complexes might be predicted to be responsive to electronic and structural differences between metal–PP substrates. This is not true for the yeast inorganic pyrophosphatase process, where rate-limiting product release appears to be important. Future studies will explore enzyme systems in which the catalytic steps and product release steps can be easily dissected.

Supplementary Material Available

A table giving the anisotropic temperature factors for the non-hydrogen atoms (1 page); a table listing all observed and calculated structure factors (10 pages). Ordering information is given on any current masthead page.

Registry No. **1**, 107053-38-3; **2** Δ, 88930-47-6; **2** Λ, 88905-07-1; MgPP, 20768-12-1; $[Rh(H_2O)_4H_2P_2O_7]^+Cl^-$, 107053-39-4; PPase, 9033-44-7; pyruvate kinase, 9001-59-6; acetate kinase, 9027-42-3; hexokinase, 9001-51-8; glycerokinase, 9030-66-4; myokinase, 9013-02-9; creatine kinase, 9001-15-4; arginine kinase, 9026-70-4; kinase (phosphorylating), 9031-44-1.

References

Bond, M. W. (1979) Ph.D. Thesis, University of Pennsylvania.

Burgess, P., & Eckstein, F. (1980) *J. Biol. Chem. 255*, 8229.

Cleland, W. W. (1985) in *Mechanisms of Enzymatic Reactions: Stereochemistry* (Frey, P. A., Ed.) pp 141–148, Elsevier, New York.

Coderre, J. A., & Gerlt, J. A. (1980) *J. Am. Chem. Soc. 102*, 6594.

Cohn, M., Shih, H., & Nick, J. (1982) *J. Biol. Chem. 257*, 7646.

Cooperman, B. S., Chia, N. Y., Bruckmann, R. H., Bunick, G. J., & McKenna, G. P. (1973) *Biochemistry 12*, 1665.

Cremer, D., & Pople, J. A. (1975) *J. Am. Chem. Soc. 97*, 1354.

Dunaway-Mariano, D. (1985) in *Mechanisms of Enzymatic Reactions: Stereochemistry* (Frey, P. A., Ed.) pp 149–164, Elsevier, New York.

Dunaway-Mariano, D., & Cleland, W. W. (1980) *Biochemistry 19*, 1506.

Eckstein, F. (1985) *Annu. Rev. Biochem. 54*, 367.

Haromy, T. P., Knight, W. B., Dunaway-Mariano, D., & Sundaralingam, M. (1982) *Biochemistry 21*, 6950.

Haromy, T. P., Knight, W. B., Dunaway-Mariano, D., & Sundaralingam, M. (1984) *Acta Crystallogr., Sect. C: Cryst. Struct. Commun. C40*, 223.

Jaffe, K. K., & Cohn, M. (1979) *J. Biol. Chem. 254*, 10839.

Janson, C. A., & Cleland, W. W. (1974) *J. Biol. Chem. 249*, 2572.

Johnson, C. K. (1976) ORTEP-II, Report ORNL-5138, Oak Ridge National Laboratory, Oak Ridge, TN.

Knight, W. B., Fitts, S. W., & Dunaway-Mariano, D. (1981) *Biochemistry 20*, 4079.

Knight, W. B., Ting, S.-J., Chuang, S., Dunaway-Mariano, D., Haromy, T. P., & Sundaralingam, M. (1983) *Arch. Biochem. Biophys. 227*, 302.

Knight, W. B., Dunaway-Mariano, D., Ransom, S., & Villafranca, J. J. (1984) *J. Biol. Chem. 259*, 2886.

Lin, I., Knight, W. B., Ting, S.-J., & Dunaway-Mariano, D. (1984a) *Inorg. Chem. 23*, 987.

Lin, I., Hsueh, A., & Dunaway-Mariano, D. (1984b) *Inorg. Chem. 23*, 1692.

Linck, C. F., Haller, K. J., & Cleland, W. W. (1986) *Fed. Proc., Fed. Am. Soc. Exp. Biol. 45*, 1648.

Merritt, E. A., & Sundaralingam, M. (1980) *Acta Crystallogr., Sect. B: Struct. Crystallogr. Cryst. Chem. B36*, 2574.

Merritt, E. A., Sundaralingam, M., & Dunaway-Mariano, D. (1981) *J. Am. Chem. Soc. 103*, 3565.

Rao, B. D. N., Buttlaire, D. H., & Cohn, M. (1976) *J. Biol. Chem. 251*, 6981.

Rao, B. D. N., Kayne, F. J., & Cohn, M. (1979) *J. Biol. Chem. 254*, 2689.

Romaniuk, P. J., & Eckstein, F. (1981) *J. Biol. Chem. 256*, 7322.

Sammons, R. D., & Frey, P. A. (1982) *J. Biol. Chem. 257*, 1138.

Schimerlik, M. I., & Cleland, W. W. (1973) *J. Biol. Chem. 248*, 8418.

Speckhard, D. C., Pecoraro, V. L., Knight, W. B., & Cleland, W. W. (1986) *J. Am. Chem. Soc. 108*, 4167.

Sundaralingam, M., & Haromy, T. P. (1985) in *Mechanisms of Enzymatic Reactions: Stereochemistry* (Frey, P. A., Ed.) pp 249–266, Elsevier, New York.

Ting, S.-J., & Dunaway-Mariano, D. (1984) *FEBS Lett. 165*, 251.

Tomasselli, A. G., & Noda, L. H. (1983) *Eur. J. Biochem. 132*, 109.

Viola, R. W., Raushel, F. M., Rendina, A. R., & Cleland, W. W. (1982) *Biochemistry 21*, 1295.